General Disclaimer

One or more of the Following Statements may affect this Document

- This document has been reproduced from the best copy furnished by the organizational source. It is being released in the interest of making available as much information as possible.

- This document may contain data, which exceeds the sheet parameters. It was furnished in this condition by the organizational source and is the best copy available.

- This document may contain tone-on-tone or color graphs, charts and/or pictures, which have been reproduced in black and white.

- This document is paginated as submitted by the original source.

- Portions of this document are not fully legible due to the historical nature of some of the material. However, it is the best reproduction available from the original submission.

JPL PUBLICATION 82-96

Precipitable Water: Its Linear Retrieval Using Leaps and Bounds Procedure and Its Global Distribution from Seasat SMMR Data

Prem Chand Pandey

December 1, 1982

NASA
National Aeronautics and Space Administration

Jet Propulsion Laboratory
California Institute of Technology
Pasadena, California

JPL PUBLICATION 82-96

Precipitable Water: Its Linear Retrieval Using Leaps and Bounds Procedure and Its Global Distribution from Seasat SMMR Data

Prem Chand Pandey

December 1, 1982

NASA
National Aeronautics and
Space Administration

Jet Propulsion Laboratory
California Institute of Technology
Pasadena, California

The research described in this publication was carried out by the Jet Propulsion Laboratory, California Institute of Technology, and was supported by the National Academy of Sciences and the National Aeronautics and Space Administration.

ABSTRACT

The Seasat Scanning Multichannel Microwave Radiometer (SMMR) measurements in the 18.0, 21.0 and 37.0 GHz channels are primarily used for precipitable water (also known as atmospheric water vapor content) and liquid water determination. Linear regressions using a leaps and bounds procedure are used for the retrieval of precipitable water. A total of eight subsets using two to five frequencies of the SMMR are examined to determine their potential in the retrieval of atmospheric water vapor content. Our analysis indicates that the information concerning the 18 and 21 GHz channels are optimum for water vapor retrieval. A comparison with radiosonde observations gave an rms accuracy of ~0.40 g/cm^2. The rms accuracy of precipitable water using different subsets was within 10 percent.

Global maps of precipitable water over oceans using two and five channel retrieval (average of two and five channel retrieval) are given. These maps are generated on a 10 day average basis as well as on a monthly basis for the period 7 July - 6 August 1978. An analysis of these global maps reveals the possibility of global moisture distribution associated with oceanic currents and large scale general circulation in the atmosphere. A stable feature of the large scale circulation is noticed. The precipitable water is maximum over the Bay of Bengal and in the North Pacific over the Kuroshio current and shows a general latitudinal pattern.

CONTENTS

Figures

Tables

1. Introduction

The Scanning Multichannel Microwave Radiometer (SMMR) on the experimental Seasat satellite, launched on 28 June 1978 and expired on 10 Oct. 1978, measured the earth's radiation at 6.6, 10.7, 18.0, 21.0 and 37.0 GHz with vertical and horizontal polarizations. These ten-channel measurements over the ocean surface can be utilized in determining the geophysical quantities: sea surface temperature, wind speed, integrated atmospheric water vapor, liquid water, and rain rate.

Recently, we [Pandey and Kakar, 1982a] have developed a two step linear statistical technique using a leaps and bounds procedure to retrieve geophysical parameters from multi-wavelength measurements. The technique has been used to estimate sea surface temperature from Seasat SMMR data. In this paper, we will use the above retrieval technique to estimate precipitable water from Seasat SMMR data. Over the open ocean three of the five SMMR frequencies on the Seasat and Nimbus-7 satellites are primarily used for determination of precipitable water.

The measurement of atmospheric water vapor and liquid water with passive microwave techniques has been made previously from earth orbit in the microwave region using 31.4, 22.2 and 19.3 GHz channels of the NEMS and ESMR radiometers on board the Nimbus-5 and the SCAMS radiometer on board Nimbus 6 [Staelin et al. 1976, Grody et al. 1980]. The SMMR has the finest spatial resolution to date (54 x 54 km) and precipitable water vapor maps of vast oceanic regions on such a fine scale is something totally new and may have great potential for future air-sea interaction research. A recent review by Njoku (1982) describes the capabilities of microwave radiometers to remotely sense meteorological and oceanographic parameters.

Precipitable water, which is defined as the depth of liquid water that would be obtained if the total amount of water vapor in a specified layer of the atmosphere above the unit area of the earth's surface were condensed into a layer on that surface, is a familiar quantity to meteorologists. Krishnamurti and Kanamitsu (1973) indicated that for short range numerical weather prediction over a global tropical belt, a detailed definition of moisture fields is extremely important. A reliable measurement and mapping of total precipitable water alone is not adequate for defining the initial state for a numerical prediction model. Haydu and Krishnamurti (1981) proposed a method for analyses of the vertical and horizontal distribution of the moisture field utilizing satellite, upper air, and surface data. The above analyses may help to use these satellite derived moisture fields for quantitative weather forecasting. In addition, knowledge of precipitable water is important in understanding the development of the tropical cyclones and cloud clusters [Ruprecht and Gray, 1976]. Moisture field distribution over the oceanic regions can help us to understand the dynamic state of the atmospheric boundary layer. Knowledge of precipitable water is also used to apply corrections with IR measurements for retrieving certain geophysical parameters such as sea surface temperature and also with Scatterometer data for correcting atmospheric attenuation while retrieving wind speed and also altimeter pathlength correction. Atmospheric circulation becomes visibly apparent only by the transport of water in the atmosphere, partly in the gaseous form and partly in liquid and solid form in clouds. The role of moisture in weather formation and in heat transport can not be undermined. The foregoing discussion thus demonstrates that moisture plays an important if not dominant role in many of the weather phenomena.

2. Retrieval with linear regressions using leaps and bounds procedure

Retrieval techniques described in the literature include, among others, statistical [Waters et al., 1975, Grody, 1976, Wilheit and Chang, 1980, Pandey et al., 1981a, Hofer and Njoku, 1981, Pandey and Kakar, 1982a], non-linear iterative [Wentz, 1982], and fourier transform techniques, the latter developed by Rosenkranz (1978). The retrieval equations discussed and used here have been derived using a two-step statistical technique described in detail by Pandey and Kakar (1982a). The technique is based upon the application of an efficient algorithm, known as 'Regressions by leaps and bounds' [Furnival and Wilson, 1974], to a statistical data base in order to select the 'best' subsets of radiometric channels. The 'best' is defined using the R^2 coefficient of determination criterion, widely used in statistical literature. Our approach is unique in the sense that it provides an opportunity to examine a number of subsets and also different subsets of the same size, which is not possible by other methods. The statistical data base consists of an ensemble of realistic sea surface temperatures, wind speeds, atmospheric water vapor profiles, temperature profiles and cloud models and are summarized in an earlier paper [Pandey and Kakar, 1982a]. Our approach of generating a data base is also slightly different than that used by earlier investigators. We have used a non-linear regression equation between water vapor and SST, which exist in nature, to generate the data base, along with other parameters. This relation was obtained from the analysis of data obtained from ocean station PAPA (50°N, 145°W) and the Monex '79 experiment. The analysis gave a value of 0.77 for the coefficient of correlation. These are used to calculate brightness temperatures by means of a surface emission model [Pandey and Kakar, 1982b] and a radiative transfer model. The retrieval equations are then obtained by using multiple linear regression on the selected subsets, based upon the statistical relationship between geophysical parameters and the calculated brightness temperatures. Non-linearity of the problem was mitigated

by using functions of brightness temperature [$f(T_B) = \ln (280-T_B)$] rather than brightness temperatures themselves, for high frequency (18.0, 21.0, 37.0 GHz) channels. Theoretical brightness temperatures were perturbed by Gaussian noise, characteristic of the SMMR instruments, which smoothed the regression coefficients and provided a more realistic approach to the problem.

The results of the leaps and bounds algorithm for selecting the best subsets of 1 to 5 channels for retrieving precipitable water are given in Table 1 along with R^2 coefficient of determination values. Four other best subsets of each size are also given in the same Table and may be used for analysis as well. This capability could be exploited to set up a quality control criterion in future algorithms as proposed in the earlier paper [Pandey & Kakar, 1982a]. Selection of the best subsets has been made from all of the 10 SMMR channels. We have dropped those subsets which selected either 6.6 or 10.6 GHz frequencies, since we are primarily interested in retrieving water vapor over a grid size of 54 x 54 km and only 18, 21 and 37 GHz data has been processed on this grid size. Table 2 gives the regression coefficients for the different subsets using 2 to 5 channels. The coefficients in Table 2 are related with functions of brightness temperature as defined earlier through the following parameter retrieval equation.

$$p_i = \sum_j a_{ij} \quad f(T_{Bj}) + a_0$$

where the (T_B)'s are functions of the brightness temperature and a_0 is the intercept. The theoretical rms error, which decreases as the number of channels increases from 2 to 5, is also shown in the Table. These theoretical rms errors are dependent upon the range of variations of the geophysical parameters used in the statistical data base and should not be directly compared with rms error obtained by other investigators.

Table 1. List of 5 best subsets of sizes one to five selected by leaps and bounds technique for deriving water vapor from SMMR channels.

Subset	Criterion $R^2 \times 100$	Variables
1	66.58	21V
	62.03	21H
	38.43	6.6V
	31.73	10.6V
	31.44	18V
2	96.62	18H, 21H
	95.95	18V, 21V
	95.18	18V, 21H
	94.00	18H, 21V
	85.06	10.6H, 21V
3	97.51	10.6H, 18H, 21H
	97.43	6.6H, 18H, 21H
	97.41	18H, 21H, 37H
	97.25	66V, 18V, 21H
	97.17	18H, 21H, 37V
4	97.81	10.6H, 18H, 21H, 37H
	97.76	10.6H, 18H, 21H, 37V
	97.74	6.6H, 18V, 18H, 21H
	97.66	6.6H, 18H, 21H, 37H
	97.63	18V, 18H, 21H, 37H
5	97.92	6.6H, 18V, 18H, 21H, 37H
	97.79	18V, 18H, 21V, 21H, 37H
	97.67	6.6V, 10.6V, 10.6H, 18H, 21H
	97.65	6.6V, 10.6V, 18V, 18H, 21H
	97.64	6.6V, 10.6V, 18H, 21H, 37H

Table 2. Regression coefficients of the selected subsets and their theoretical rms error. Function of brightness temperature [$f(T_B)=\ln(280-T_B)$] is used.

Subset Size	Intercepts	Regression coefficients 18 V	18 H	21 V	21 H	37 V	37 H	rms error g/cm^2
2	-15.6652	13.2287	-	-9.9410	-	-	-	.38
2	-16.0639	-	11.1811	-8.8038	-	-	-	.46
2	-19.1256		14.5305	-	-10.8518	-	-	.35
2	-15.1272	16.0135	-	-	-11.7677	-	-	.42
3	-16.0979		13.7272	-	-10.9226	1.3276		.32
3	-14.5772		13.1278		-10.8864	-	1.5689	.30
4	-14.4035	4.2409	9.5939	-	-11.2576	-	.5490	.29
5	-13.5842	7.0862	6.2669	-2.9281	-8.0304	-	.5657	.28

3. Bias determination and comparison with Chester's algorithm

Before comparing satellite derived water vapor with radiosonde observations we compared the retrieval of water vapor using different subsets with that of Chester's algorithm [Lipes and Born, 1981]. Chester's algorithm is being used at Jet Propulsion Laboratory for geophysical processing of Seasat SMMR data. Two-hundred data points selected from descending revolutions for the period September 16-22, 1978 were used for comparison. These revolutions covered the latitude belt of +50° to -50° over the Pacific and provided a wide range (1.0 to 6.5 g/cm^2) of variations of water vapor for comparison. The results of the comparison are presented in Table 3. The bias varied from -.05 to 1.7 g/cm^2 for different subsets and the rms difference varied from 0.10 g/cm^2 to 0.24 g/cm^2.

Chester's algorithm, given in the Appendix, depends heavily on Wilheit and Changs' (1980) earlier work, and has been tuned empirically to obtain agreement between retrieved and measured water vapor. The precipitable water obtained using the regression equation derived from radiative transfer calculations is thus modified empirically depending upon whether the value of the retrieved precipitable water is greater than or less than 5.67 g/cm^2. No such empirical adjustment has been made in our regressions, thus, basic physics has been preserved in our approach. In addition, we have not used incidence angle as an additional predictor as has been done in Wilheit and Changs' approach.

4. Comparison with radiosonde measurements

The regression whose coefficients are given in Table 2 were corrected for biases given in Table 3. These corrected regression equations were then used for retrieving water vapor and were compared with radiosonde observations. This procedure was adopted for bias correction so that more data sets would be available for comparison. Comparison of precipitable water against radiosonde data is obviously difficult since the radiosonde network is widely scattered

Table 3. Summary of Comparison of SMMR-derived water vapor and biases using different subsets with Chester's algorithm. Two-hundred data points over Pacific during the month of September were used for comparison.

Channels of the subsets	rms difference g/cm^2	Bias g/cm^2
18V, 21H	0.15	1.71
18V, 21V	0.19	0.57
18H, 21V	0.24	-.05
18H, 21H	0.11	.88
18H, 21H, 37V	0.13	0.92
18H, 21H, 37H	0.13	0.89
18V, 18H, 21H, 37H	0.13	1.12
18V, 18H, 21V, 21H, 37H	0.10	0.98

throughout the tropical Pacific ocean. Table 4 shows the stations used to collect the verification data for comparison with Seasat SMMR precipitable water. Software for match-ups was developed and 62 pairs of coincident in-situ and satellite observations were picked. A match between the two data sets is assumed when the satellite field of view is within ± 0.5° latitude and longitude of the radiosonde (raob) station location and when the time difference between the radiosonde launches and satellite passes is within ± 3 hours of radiosonde launches. We believe that this has provided high quality ground truth for comparison, although data points could have been increased by relaxing the above match-up criteria. The results of the comparison of retrieved water vapor using different subsets are presented in Table 5. It is interesting to observe from Table 5, that all of the retrievals agree within ± 10% with negligible bias. Thus any subsets using two to five channels could be used for water vapor retrieval. It is important to note that the addition of high frequency channels (37 GHz) has not improved the water vapor retrieval over two-channel retrieval. Chester's algorithm gives an rms error of 0.37 g/cm^2 which is not significantly different than that obtained by using two to five frequency subsets. As an example, the scatter plot of two frequency retrieval (18, 21) vs in-situ observations is shown in Figure 1. The rms difference is 0.44 g/cm^2. This rms difference compares favorably with theoretical rms error (Table 2). The theoretical rms error with more channels is better (but not significantly) as can be seen from Table 2, but the rms error obtained with radiosonde comparison is greater by a factor of 2 than the theoretical estimate. However, it compares favorably with 0.44 g/cm^2 rms error obtained by Staelin et al. (1976) and 0.50 g/cm^2 rms error obtained by Grody et al. (1980), using 22 and 31 GHz channels from Nimbus 5 and Nimbus 6 satellites. Not a single data point has been filtered in the present analysis. The range of variation of precipitable water was found to be ~3 - 6.5 g/cm^2.

Table 4. List of radiosonde (Raob) stations and measured radiosonde observations used in the comparison presented in Table 5.

Raob Station	Date	Raob location and precipitable water			
		Lat	Long	Time	H_2O Vapor g/cm^2
Funafuti	9-10-78	-8.52	179.22	2300	4.7
	9-13-78			2300	3.8
	9-16-78			2300	3.2
	9-22-78			2300	6.4
	9-25-78			2300	3.9
	9-28-78			2300	5.4
	10-1-78			2300	6.3
Guam	9-13-78	13.55	144.83	2300	5.4
	9-16-78			2300	5.0
	9-28-78			2300	6.0
Kwajalein	9-10-78	8.72	167.73	2300	5.5
	9-28-78			2300	5.0
Majuro	9-19-78	7.03	171.38	2300	4.5
	9-16-78			2300	6.1
	9-25-78			2300	5.2
	9-28-78			2300	5.5
Tango	9-17-78	29.0	135.00	0000	4.7
	9-23-78			0000	5.8
	9-26-78			0000	3.5
	9-29-78			0000	4.1
Truk	9-24-78				
	10-2-78	7.45	151.85	2300	6.4
				2300	5.9
Wake Island	9-10-78	19.28	16665	2300	5.0
	9-13-78			2300	5.3
	9-16-78			2300	3.6
	9-28-78			2300	5.5
	10-1-78			2300	4.7

Table 5. Summary of the results of comparison of radiosonde and SMMR-derived values of total precipitable water using different subsets. Sixty-two data points were used in the comparison.

Channels of the subset	rms error g/cm^2	Bias g/cm^2
18V, 21H	.44	.08
18V, 21V	.40	.02
18H, 21V	.44	-.04
18H, 21H	.44	.09
18H, 21H, 37V	.44	.10
18H, 21H, 37H	.44	.11
18V, 18H, 21H, 37H	.43	0.12
18V, 18H, 21V, 21H, 37H	.40	0.10
Chester's algorithm	.37	-.04

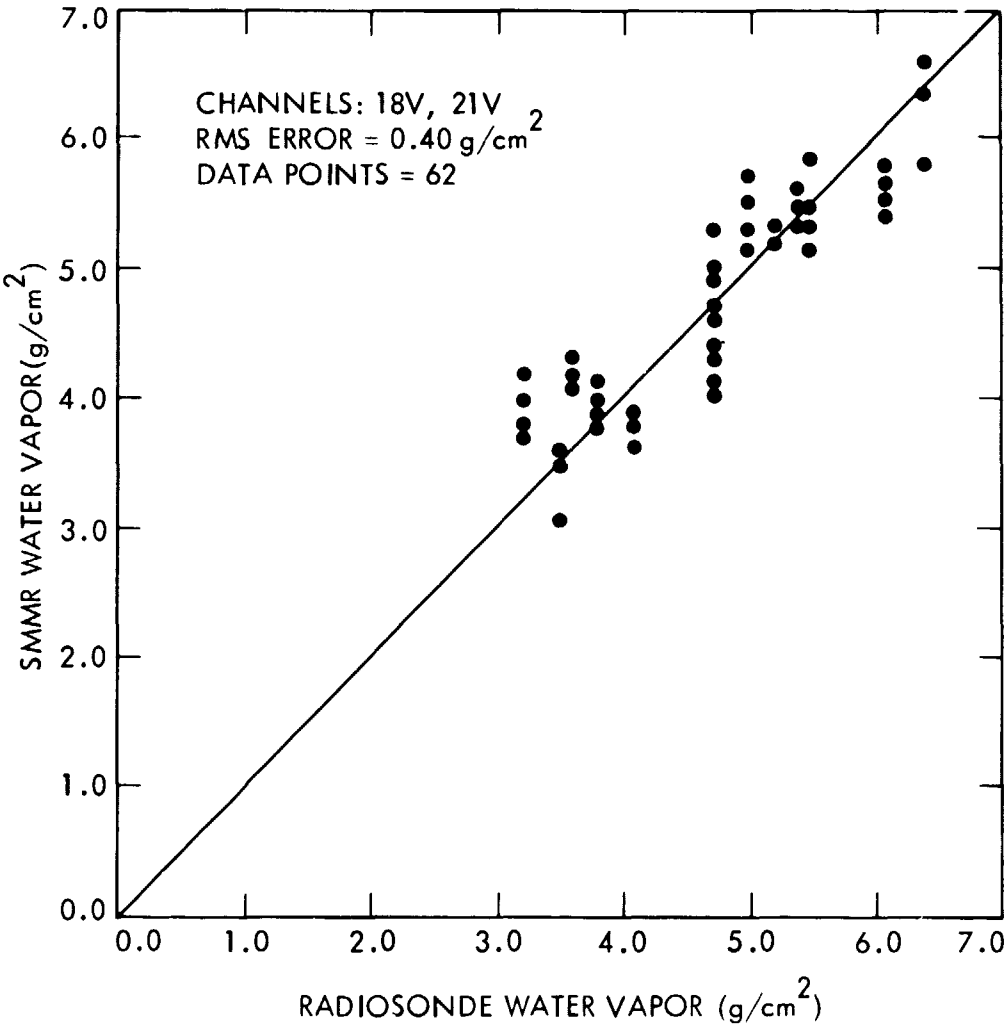

Fig. 1. Comparison of precipitable water derived from Seasat SMMR and nearby radiosonde for the month of September 1978

The remarkable agreement between the retrievals using different frequency subsets demonstrates beyond doubt the quality of Seasat SMMR data (at least high frequency channels) for the retrieval of water vapor.

5. Approximately 10-day and mean monthly global maps of precipitable water

In our approach of generating global maps of precipitable water, the brightness temperature data were used to obtain water vapor (WV) using a linear two and five channel algorithm as described earlier. An average of the two retrievals provided the WV. These parameters were then interpolated to a fixed 2° x 2° latitude-longitude grid for the entire globe for further analysis. Since the algorithm is applicable only to sea surfaces, any data near land will produce error and should be avoided. The interpolated values of WV at each grid point were obtained using a weighted average of all data within a 2° radius of influence for each grid point according to

$$WV = \frac{\sum W_i \times WV_i}{\sum W_i}$$

The weighting factor W_i assigned to the individual data values are given by the Cressman formula

$$W_i = \frac{D^2 - d_i^2}{D^2 + d_i^2} \quad d_i < D$$
$$= 0 \quad d_i > D$$

where D is the 2° radius of influence and d_i is the distance of each data point from the grid position. The uniform grid of WV created by this weighting process was used as input for the contour package. The software used to generate these contour plots was developed by Chelton at Jet Propulsion Laboratory and implemented on a Digital VAX 11/780 using the Pilot Ocean Data System. It should be noted that Chelton's program uses a "box filter" method of smoothing the data in which

the contents of a box surrounding the point of interest are averaged to derive a new grid value. In the contour plots presented here a 6° x 2° box filter was used (Figures 2, 3, 4, and 5).

The Seasat SMMR data at grid 3 was analyzed for generating global maps of water vapor. These data are given in Table 6. Three approximately 10-day period maps and one for the period of one month (7 July to 6 Aug. 1978) were generated and they are given in Figures 2, 3, 4, and 5. These maps give a good representation of the atmospheric moisture distribution connected with different elements of the atmospheric circulation over both hemispheres.

An examination of the precipitable maps shows that maximum moisture is obtained over the Bay of Bengal and in the North Pacific over the Kuroshio current which conform to the findings of Tuller (1968) based on the sparsely available radiosonde data. A latitudinal dependence of moisture distribution is also seen from the maps. The ten day maps showing time variation and also the mean monthly map show the stable seasonal features of the atmospheric circulations. Such stable seasonal features were also noticed by Mitnik (1971) from radiometric measurements aboard the Cosmos-243 satellite. The global maps show some basic differences in the distribution of moisture over the northern and southern hemispheres, largely due to their differing distributions of land and water. The maximum of precipitable water associated with the Intertropical Convergence Zone (ITCZ) is noticeable both to the north and south of the equator.

In the Indian ocean, the moisture distribution over the central part and eastern part is higher than the western part due probably to the cold current (Mozambique current) flowing near the east African coast. Again, in the central and eastern part of the Indian ocean the isolines show latitudinal behaviour whereas in the western part they show meridional tendency. A strong moisture gradient is also evident in the central part of the Indian ocean. The moisture distribution over the Bay of Bengal is higher than the Arabian sea, possibly

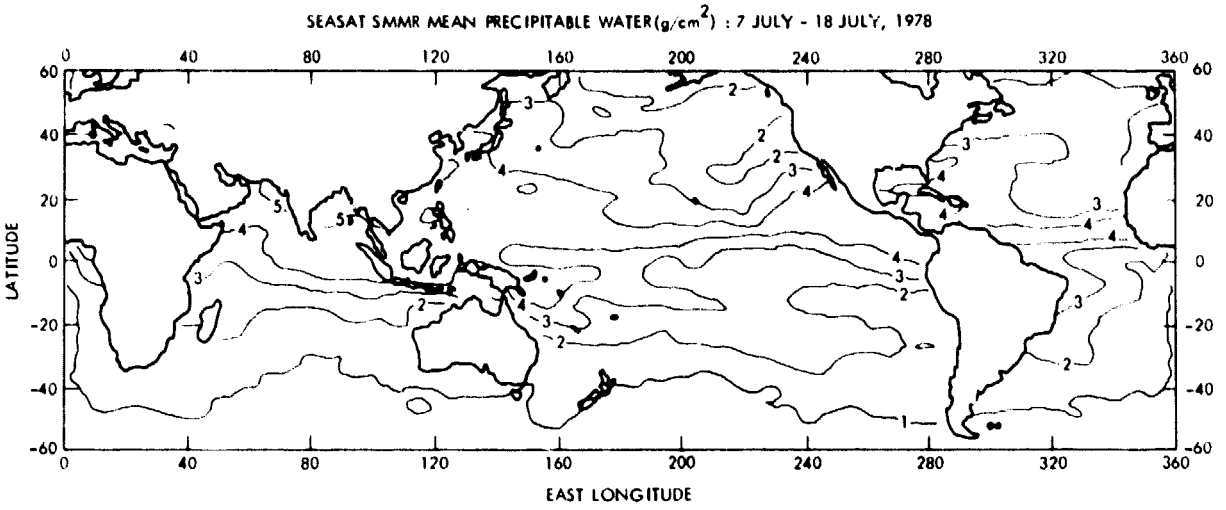

Fig. 2. Global SMMR moisture field for the period 7 July - 18 July, 1978

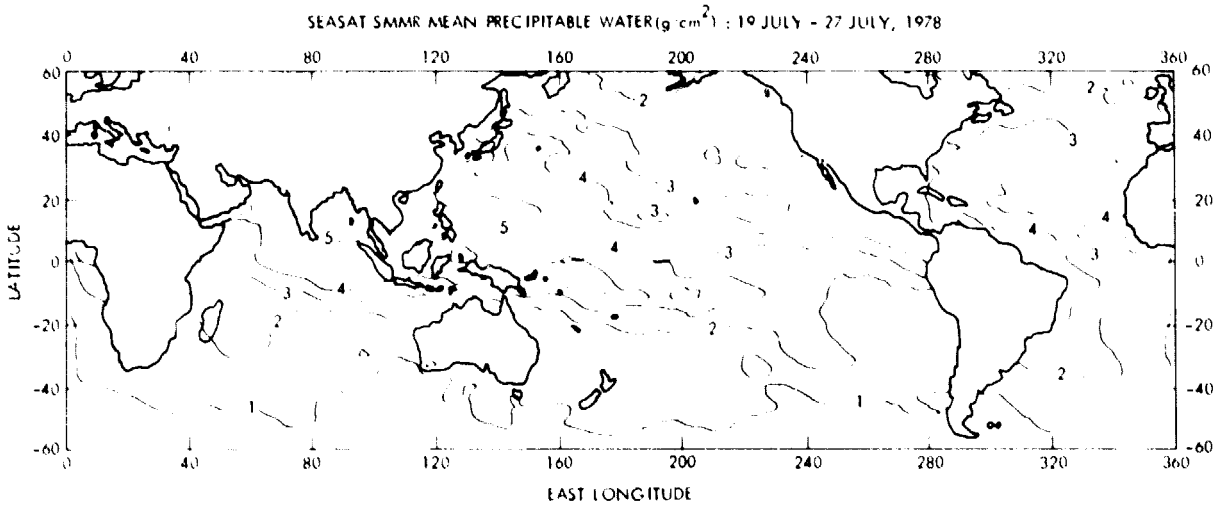

Fig. 3. Global SMMR moisture field for the period 19 July - 27 July, 1978

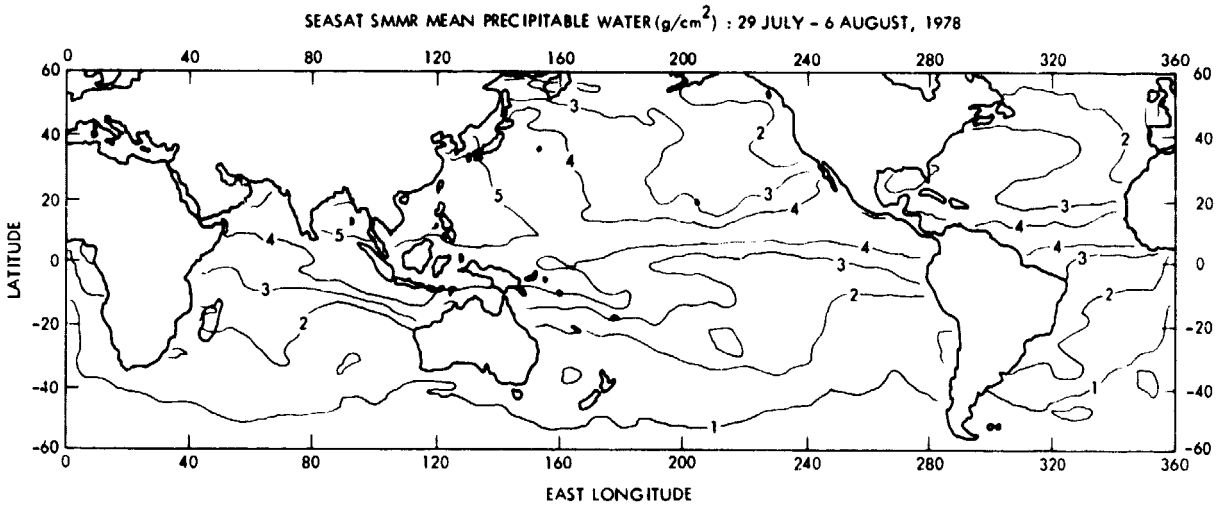

Fig. 4. Global SMMR moisture field for the period 29 July - 6 August, 1978

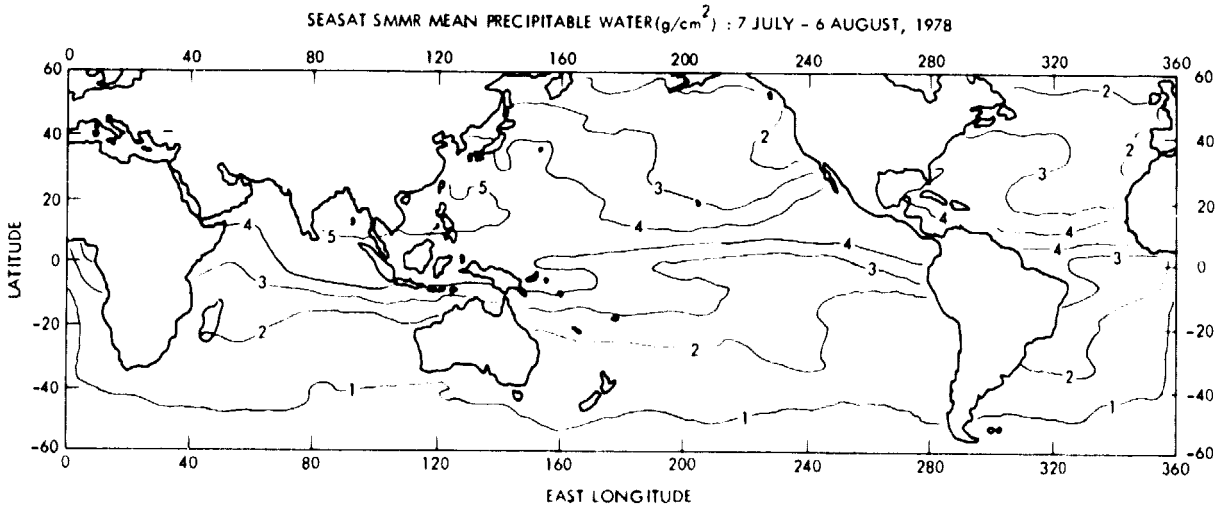

Fig. 5. Global SMMR mean monthly moisture field for the period 7 July - 6 August, 1978

TABLE 6. Summary of the Seasat revolutions used in generating the moisture fields.

Orbit No.	Date	Times	Equator Crossing °E
147	7 July 78	0744-0754	137.8
175	9 July 78	0639-0650	155.5
204	11 July 78	0718-0727	148.1
218	12 July 78	0648-0652	156.9
233	13 July 78	0756-0807	140.6
262	15 July 78	0834-0845	133.3
276	16 July 78	0803-0814	142.1
290	17 July 78	0733-0735	151.0
304	18 July 78	0701-0712	159.8
319	19 July 78	0810-0821	143.5
333	20 July 78	0737-0753	152.4
458	21 July 78	0848-0902	136.1
362	22 July 78	0816-0831	145.0
376	23 July 78	0745-0759	153.8
390	24 July 78	0713-0727	162.6
391	24 July 78	0854-0908	137.6
405	25 July 78	0824-0838	146.4
419	26 July 78	0752-0806	155.2
433	27 July78	0720-0734	164.1
434	27 July 78	0901-0915	139.0
462	29 July 78	0759-0813	156.7
477	30 July 78	0909-0922	140.5
505	1 Aug 78	0806-0820	158.1
520	2 Aug 78	0915-0930	141.9
534	3 Aug 78	0845-0859	150.7
548	4 Aug 78	0813-0828	159.6
549	4 Aug 78	0953-1007	134.5
563	5 Aug 78	0922-0936	143.4
577	6 Aug 78	0851-0906	152.2

because of the higher sea surface temperature of the Bay of Bengal. The same feature has been noticed by Pandey et al. (1981b) from the analysis of total water vapor from the Second Indian Satellite Bhaskara. In the southern hemisphere, a mass of dry air (moisture between 1-2 g/cm^2) is observed below 20°s.

In the Pacific ocean, it is seen from the moisture distribution map that the air in the northern hemisphere is more moist than in the southern hemisphere. In the northern hemisphere, a large meridional moisture gradient is observed near the California current and its counterpart in the southern hemisphere is on the western side of South America where the Peru or Humboldt current flows equatorward. In the western part of the Pacific, a 'tongue' of moist air is clearly seen in both the northern and southern hemisphere. The oceanic circulation is influenced by the subtropical oceanic high pressure circulation that is centered approximately 40°N, 150°W and also by westerlies. Equatorward of the subtropical high pressure cells, persistent trade winds generate the broad north and south equatorial current (~10° latitude N and S) and moisture isolines follow zonal trends. This is because of the general similarity between wind fields and general oceanic circulation [Tabata, 1975]. On the western side of the oceans, most of the water swings poleward with airflow and increasingly comes under the influence of the Ekman deflection and the anticyclonic vorticity effect causing the 'tongue' of moist air in the northern hemisphere, with a similar 'tongue' in the southern hemisphere. On the poleward side of the subtropical high pressure cells, westerly currents dominate, and where they are unimpeded by landmasses in the southern hemisphere, they form the broad Antarctic Circumpolar Current.

In the Atlantic ocean, as in the Pacific, the moisture in the northern hemisphere is greater than in the southern hemisphere. Zonal distribution of isolines is concentrated within a region of 0-20°N latitude, and is more pronounced in the mean monthly maps. The 'tongue' of moist air is more marked in the

northern hemisphere than in the southern hemisphere. The isolines of 4 g/cm^2 and 3 g/cm^2 join the fast and narrow Gulf Stream which flows poleward in the North Atlantic. In the southern hemisphere the isolines of 3 g/cm^2 and 2 g/cm^2 join the Brazil and Falkland currents in the western South Atlantic. Most of these characteristics were revealed in earlier studies [Grody et al. 1980, Prabhakara et.al. 1982] but not on such fine scale.

6. CONCLUSIONS:

This study indicates that retrieval of a given geophysical parameter with linear regressions using leaps and bounds procedure is an important strategy when the goal of the experimentation is prediction and costs of the instrumentation involved are high. An analysis of the eight subsets using two to five frequencies of Seasat SMMR demonstrates that it is possible to achieve the accuracy of radiosondes (10%) in deriving precipitable water. The information content of the 18 and 21 GHz brightness temperature data appears to be optimal of SMMR for water vapor retrieval. For the data sets considered in the present investigation no substantial improvements are obtained using a larger number of channels for water vapor retrieval. However, it is possible to improve the accuracy of water vapor retrieval further by using different subsets either of the same size or of different sizes by imposing a quality control criterion such that retrieval from a given subset does not differ from retrievals with other subsets from a predetermined threshold value. This ability of the retrieval technique to recognize severe noise in brightness temperature measurements that may lead to unacceptable parameter retrieval has not been investigated in the present paper.

It has now been possible to display the water vapor variability on a much finer scale than that possible with earlier satellites. The analysis of the global maps of water vapor shows that distribution is not an isolated phenomenon

but is closely related to ocean currents and atmospheric circulation. Most of these distribution characteristics conform to the earlier studies [Grody et al. 1980, Prabhakara et al. 1982] using microwave and IR satellite data, though of course on a much coarser resolution for microwaves.

Although precipitable water as such is not usable for numerical weather prediction, it has been used in an objective analysis by Haydu and Krishnamurti (1981) to obtain a moisture profile. Also, an attempt is underway to develop instruments with channels around the 183 GHz water vapor line in addition to the more transparent line at 22 GHz for obtaining moisture profile information. Additional knowledge of precipitable water may help to improve the retrieval of moisture profile from 183 GHz data. As our understanding about the ocean-atmosphere system improves, these parameters may find new applications in the future.

ACKNOWLEDGEMENTS

J. W. Waters, E. G. Njoku, R. K. Kakar and D. Chelton are gratefully acknowledged for their comments on the manuscript. Stacy Kniffen, a graduate student from Texas A & M University, College Station, Texas, helped in programming. Dudley Chelton allowed the use of his software package for contour plotting on the VAX-11/780 computer system. Stephanie Gallegos provided assistance in manuscript preparation and Bonnie S. Beckner provided excellent typing, for which they are gratefully acknowledged. Prem C. Pandey thanks the National Research Council for his associateship during the research reported in this paper.

Dr. Pandey is on leave from the Space Applications Centre (ISRO), Ahmedabad-380053, India.

REFERENCES

Furnival, G.M. and R.W. Wilson, Jr., 1974: Regressions by leaps and bounds, Technometrics, vol 16, pp 499-511

Grody, N.C., 1976: Remote sensing of atmospheric water content from satellites using microwave radiometry, IEEE Trans. Antennas Propagat., AP-24, 155-162

Grody, N.C., A. Gruber and W.C. Shen, 1980: Atmospheric water content over the tropical Pacific derived from the Nimbus-6 Scanning Microwave Spectrometer. J. Appl. Met. 19, 986-996

Hofer, R. and E.G. Njoku, 1981: Regression techniques for oceanographic parameter retrieval using spaceborne microwave radiometry, IEEE Geoscience and Remote Sensing, vol GE-19, pp 178-189

Haydu, K.J. and T.N. Krishnamurti, 1981: Moisture analysis from radiosonde and microwave spectrometer data, J. Appl. Met. 20, 1177-1191

Krishnamurti, T.N. and M. Kanamitsu, 1973: A study of a coasting easterly wave, Tellus, 25, 568-586

Mitnik, L.M., 1971: Measurement of water vapor content over the oceans by SHF radiometers aboard COSMOS-243, Advances in Satellite Meteorology, Wiley and Sons, New York

Njoku, E.G., 1982: Passive microwave remote sensing of the earth from space - A review, Proc. IEEE vol. 70, pp 728-750

Pandey, P.C. and R.K. Kakar, 1982a: A two step linear statistical technique using leaps and bounds procedure for retrieving geophysical parameters from microwave radiometric data, IEEE J. of Geoscience and Remote Sensing (in press)

Pandey, P.C. and R.K. Kakar, 1982b: An empirical microwave emissivity model for a foam covered sea, IEEE J. of Oceanic Eng. OE-7, pp 135-140

Pandey, P.C., A.K. Sharma and B.S. Gohil, 1981a: A simulation technique for the determination of atmospheric water content with Bhaskara Satellite Microwave Radiometer (SAMIR), Proc. Ind. Acad. of Science (Earth Planet. Science), 90, pp 105-110

Pandey, P.C., B.S. Gohil and A.K. Sharma, 1981b: Remote sensing of atmospheric water content from satellite microwave radiometer (SAMIR) on Bhaskara, Mausam, vol 32, pp 17-22

Prabhakara, C., H.D. Chang and A.T.C. Chang, 1982: Remote sensing of precipitable water over the oceans from Nimbus 7 microwave measurements, J. Appl. Meteor., 21, pp 59-68

Rosenkranz, P.W., 1978: Inversion of data from diffraction limited multiwavelength remote sensors, 1. linear case, Radio Science, 13, 1003-1010

Lipes, R.G. and C.H. Born, Eds, 1981: SMMR Mini-Workshop IV, Jet Propulsion Laboratory, California Institute of Technology, Pasadena, California 91109, Report No. 622-234 (internal document)

Ruprecht, E. and W.M. Gray, 1976: Analysis of satellite observed tropical cloud clusters, II. Thermal, moisture and precipitation. Tellus, 23, pp 414-425

Staelin, D.H., K.F. Kunzi, R.L. Pettyjohn, R.K.L. Poon, R.W. Wilcox and J.W. Waters, 1976: Remote sensing of atmospheric water vapor and liquid water with the Nimbus 5 microwave spectrometer, J. Appl. Met. 15, 1210-1214

Tabata, S., 1975: The general circulation of the Pacific ocean and a brief account of the oceanographic structure of the north Pacific ocean, Part I. Circulation and volume transport, Atmosphere 13, pp 135-168

Tuller, S.E., 1968: World distribution of mean monthly and annual precipitable water, Mon Weath. Rev. 96, 785-797

Waters, J.W., K.F. Kunzi, R.L. Pettyjohn, R.K.L. Poon, and D.H. Staelin, 1975: Remote sensing of atmospheric temperature profile with Nimbus 5 microwave spectrometer, J. Atm. Sci. 32, 1953-1969

Wilheit, T.T. and A.T.C. Chang, 1980: An algorithm for retrieval of ocean surface and atmospheric parameters from the observations of the scanning multichannel microwave radiometer, Radio Science, 15, pp 525-544

Wentz, F.J., 1982: Model function for ocean microwave brightness temperature, J. Geophys. Res. (in press)

APPENDIX

Chester's Water Vapor Algorithm

The water vapor algorithm is almost identical to that of Wilheit and Chang [1980]. This formula is

$$V = -9.784 + 6.927 \ln (280 - T_{18V}) + 5.361 \ln (280 - T_{18H})$$

$$-4.518 \ln (280 - T_{21V}) - 6.081 \ln (280 - T_{21H}) + 0.03890 \ (g/cm^2)$$

The modification is

$$V' = V - 1.17, \qquad V > 5.67$$

$$= 0.88(V - 1.17) + 0.56, \qquad V < 5.67$$

The bias removal of 1.17 made retrievals of large water vapor values unbiased and the linear correction prevented the underestimate of small water vapor values.